PERGAMON

Carbon 41 (2003) 945–950

CARBON

Effect of the pitch-based carbon anode on the capacity loss of lithium-ion secondary battery

Weiming Lu, D.D.L. Chung*

Composite Materials Research Laboratory, University at Buffalo, State University of New York, Clifford C. Furnas Hall, Box 60440, Buffalo, NY 14260-4400, USA

Received 27 January 2001; accepted 21 November 2002

Abstract

The total capacity loss of lithium-ion secondary cell is reduced by engineering the pitch-based carbon anode through one or more of the following methods: attaining a high degree of graphitization, minimizing the surface oxygen concentration, attaining a large crystal size L_c, degassing, and use of PVDF in place of teflon as the binder.

Keywords: A. Pitch, Electrodes; B. Activation; C. Photoelectron spectroscopy; D. Electrochemical properties

1. Introduction

The lithium-ion battery is a secondary battery, as it is rechargeable. The rechargeability avoids pollution resulted from the discarding of used batteries that are not rechargeable. Furthermore, the secondary battery is a renewable and clean source of energy. However, the technology suffers from the irreversible capacity after the first charge–discharge cycle, due to the irreversible reactions that occur during the first cycle. After the first cycle, the reversibility is better, due to the formation of a passivation layer on the carbon anode during the first cycle. The structure and surface chemistry of the carbon anode have much effect on the irreversible capacity, in addition to affecting the reversible capacity [1–11]. In particular, a high concentration of oxygen-containing functional groups is not desirable [12].

Three types of carbon have been used as the anode in the Li-ion secondary battery. They are soft carbons (e.g. pitch-based carbons), hard carbons (e.g. polymer-based carbons) and graphitic carbons. Among these, hard carbons were used in industries and remain attractive in research due to their relatively low irreversibility and high energy density. Graphitic carbons are widely used due to their high efficiency and low cost. Soft carbons have received attention because of their high energy density and low cost, but they suffer from high irreversibility. Therefore, it is highly desirable to decrease the irreversibility of soft carbons, although this is desirable for all carbons. This work is aimed at this by the use of heat treatment (carbonization and graphitization) for bulk structural control and surface treatment (degassing, activation and reduction in H_2) for control of the surface structure and chemistry. In addition, this work addresses the effect of the binder (teflon [4,8] vs. polyvinylidene fluoride [1,2,5,6,10]) in the carbon anode on the charge/discharge composites.

2. Experimental

The pitch-based carbon was obtained by heat treating mesophase pitch from the Institute of Coal Chemistry, Chinese Academy of Sciences, Taiyuan, China. The heat treatment (for 30 min at temperature) was conducted for carbonization/graphitization at 600–1100 °C in N_2, with a heating rate of 20 °C min^{-1}, or at 1200–3000 °C in argon, with a heating rate of 50 °C min^{-1}. Subsequent to heat treatments up to 1100 °C, activation was performed in CO_2 at 970 °C for either 15 or 20 min, followed by reduction in H_2 at 800 °C.

In order to investigate the effect of various steps of the

*Corresponding author. Tel.: +1-716-645-2593; fax: +1-716-645-3875.

E-mail address: ddlchung@acsu.buffalo.edu (D.D.L. Chung).

0008-6223/02/$ – see front matter
doi:10.1016/S0008-6223(02)00435-9

treatment, the following six types of samples were evaluated. Sample 1 was obtained by heating mesophase pitch at 700 °C. Sample 2 was obtained by heating mesophase pitch at 1100 °C. Sample 3 was obtained from sample 2, followed by activation at 970 °C for 20 min. Sample 4 was obtained from sample 2 by activation at 970 °C for 15 min. Sample 5 was obtained from sample 4 by reduction in H_2 at 800 °C. Sample 5′ was the same as sample 5, except that the sample was not in contact with air after reduction and before analysis.

Specimens left in air for a week or more were subjected to degassing by heating in vacuum at 150 °C for 1 h. The effect of degassing on the electrochemical performance was evaluated.

Two different grades of petroleum-based mesophase pitch (labeled A and B) were used. The resulting carbon samples are accordingly labeled samples A-1, A-2, A-3, A-4, A-5 and A-5′ for the samples derived from pitch A, and labeled samples B-1, B-2, B-3, B-4 and B-5 for the samples derived from pitch B. Both pitches A and B had 100% anisotropic content. The softening points were 289 and 246 °C for pitches A and B, respectively. The difference in softening point suggests differences in domain size and molecular weight distribution. The resulting carbons in bulk form were subjected to ball milling for the purpose of converting them to powder form.

The samples listed above were analyzed by X-ray diffraction (XRD) in order to determine the *c*-axis crystal size L_c and the interlayer spacing d_{002}. A Siemens X-ray diffractometer, with Cu Kα radiation, was used. The 2θ scan rate was $0.02° s^{-1}$.

The samples were also analyzed by electron spectroscopy for chemical analysis (ESCA) in order to observe the surface functional groups and to characterize them in terms of their type and concentration. In particular, oxygen-containing functional groups were indicated by the C1s binding energy, which is 284.77, 286.20, 287.70 and 289.10 eV for $-\overset{|}{\underset{|}{C}}-$, $-\overset{|}{\underset{|}{C}}-O$, $>C=O$, and $-\overset{||}{C}-O$, respectively. In this paper, $>C=O$, and $-\overset{||}{C}-O$ were considered together as C=O. Monochromatized Al Kα X-ray was used, with a spot size of 1000 μm.

The samples were also analyzed by N_2 adsorption at 77 K, using the ASAP 2010 analyzer from Micromeritics (Norcross, GA, USA), in order to determine the BET specific surface area. Specimens were degassed in vacuum at 150 °C for 1 h prior to adsorption analysis.

Electrochemical charge–discharge cycling testing was conducted in a dry box filled with argon gas, using the various samples of carbon as the anode material. The carbon working electrode was prepared by (i) degassing the carbon powder in vacuum at 150 °C for 1 h, (ii) mixing the carbon powder (96 wt%), the binder (4 wt%, teflon as the binder unless stated otherwise) and ethanol to form a paste, (iii) making a foil from the paste, (iv) cutting a disc from the foil, (v) pressing the disc at a pressure of 30 $kg\,cm^{-2}$, and (vi) drying the disk in vacuum at 125 °C. Step (i) is optional and is for removing the adsorbed moisture, oxygen and other volatile species from the surface of the carbon powder. Step (i) was not performed, unless stated otherwise.

A three-electrode teflon T-cell, with three steel rods to serve as support of the three electrodes, was used (Fig. 1). Both reference and counter electrodes were lithium metal foils. The electrolyte was a 1 M solution of $LiPF_6$ in a 1:1 (by volume) solution of ethylene carbonate (EC) and diethyl carbonate (DEC). Microporous polypropylene (Celgard 2500, Hoechst Celanese Corp., Charlotte, NC, USA) was used as the separator. The cell was evacuated and then backfilled with the electrolyte in order to degas the porous separator and impregnate it with the electrolyte. Electrochemical measurement involved galvanostatic cycling at a constant current density of 0.25 $mA\,cm^{-2}$ and a potential between 0 and 2.0 V Li/Li^+. The first charge/discharge cycle was studied, with focus on the effect of the carbon material.

The effect of the binder in the carbon anode was studied by comparing the electrochemical performance of carbon anodes prepared with the teflon binder and those prepared with the polyvinylidene fluoride (PVDF) binder. Both

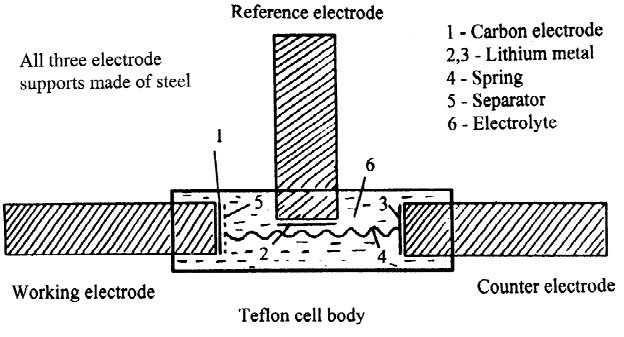

Fig. 1. Charge/discharge test cell configuration.

binders are in the form of particles. The particle size is 1 μm for teflon and 5 μm for PVDF.

3. Results and discussion

Table 1 gives the structural information on the carbons, as determined by ESCA, BET and XRD. The A and B samples are structurally similar, though there is a small difference in L_c. Activation (samples 3 and 4) increases the concentrations of both C–O and C=O functional groups on the carbon surface for both A and B samples. Reduction in H_2 (sample 5) after activation decreases these concentrations and increased the C–H concentration. The BET specific surface area is increased by activation and is not changed upon subsequent reduction in H_2. The crystallographic parameter d_{002} seems to be increased and L_c seems to be decreased by activation, but the effects are negligibly small. Both parameters are not changed upon subsequent reduction in H_2.

Table 2 shows the effect of the heat-treatment temperature on the first charge/discharge capacities of carbons based on pitch A. The total capacity loss is defined as:

$$\text{Total capacity loss} = \frac{\text{Charge capacity} - \text{Discharge capacity}}{\text{Charge capacity}}$$

Both the charge capacity and the total capacity loss are outstandingly high for the low heat-treatment temperature of 600 °C. However, both quantities decrease much with increasing heat-treatment temperature. The charge capacity advantage of a low heat-treatment temperature (below about 700 °C) is consistent with previous work on pitch-based carbons [13].

For the heat-treatment temperature of 3000 °C, the discharge capacity decreases gradually upon charge/discharge cycling. At the 20th cycle, the discharge capacity is 11% less than that at the first cycle, and is 5.7% less than that at the third cycle. Fig. 2 shows the first charge (Li deintercalation) and first discharge (Li intercalation) characteristics of the carbon based on pitch A, with a heat-treatment temperature of 3000 °C.

Table 2
First charge/discharge capacities of carbons based on pitch A

Heat-treatment temperature (°C)	Charge/discharge capacity (mAh g^{-1})	Total capacity loss (%)
600	1160/446	62
700	832/452	46
1200	564/328	42
2400	381/290	24
3000[a]	392/309	21

Total capacity loss = (first charge capacity − first discharge capacity)/first charge capacity.

[a] Third discharge capacity: 290.9 mAh g^{-1}; 20th discharge capacity: 274.3 mAh g^{-1}.

Fig. 3 shows the characteristics during first charge (C1), first discharge (D1) and second charge (C2) of samples A-1, A-2, A-3, A-4, A-5 and A-5′. The corresponding first charge/discharge capacities and total capacity loss are shown in Table 3. The increase of the heat-treatment temperature from 700 °C (sample A-1) to 1100 °C (sample A-2) substantially decreases the charge capacity and the total capacity loss. Activation (samples A-3 and A-4) increases both charge and discharge capacities, such that the increase is less for a shorter activation time (sample A-4). Reduction in H_2 after activation (samples A-5 and A-5′) decreases the charge capacity and the total capacity loss, such that the decrease is more for the case of no air contact after reduction (sample A-5′). Hence, controlled activation is useful for increasing the charge and discharge capacities, though the consequent increase in surface oxygen concentration (Table 1) is not desirable for reducing the total capacity loss. Subsequent reduction in H_2 decreases the surface oxygen concentration (Table 1),

Table 1
Structural information on the carbon samples

Sample no.	C–H	C–O	C=O	BET (m^2 g^{-1})	d_{002} (Å)	L_c (Å)
A-1	96.2	3.8	0	1.2	3.39	61
A-2	97.4	2.6	0	0.9	3.38	62
A-3	91.4	6.2	2.4	56.2	3.40	59
A-4	93.2	5.7	1.1	19.2	3.40	59
A-5	96.7	3.1	0.2	19.2	3.40	59
A-5′	–	–	–	19.2	3.40	59
B-1	96.2	3.8	0	1.2	3.39	71
B-2	97.5	2.5	0	0.9	3.38	74
B-3	91.6	6.1	2.3	56.2	3.40	68
B-4	93.2	5.7	1.1	19.2	3.40	69
B-5	96.7	3.1	0.2	19.2	3.40	69

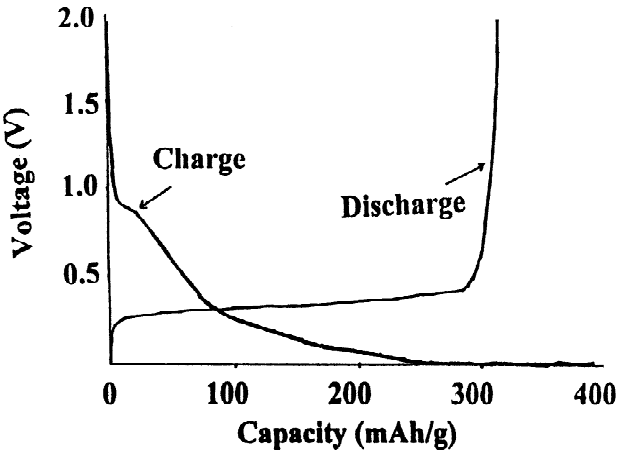

Fig. 2. First charge/discharge characteristics of carbon based on pitch A, with a heat-treatment temperature of 3000 °C.

thereby reducing the total capacity loss. However, the reduction is highly effective only if the specimen is not allowed to contact air after the reduction step.

The reversible capacity shown in Table 3 was given by R in Fig. 3, as obtained by removal of the Li plating region P shown in Fig. 3. Controlled surface modification resulted in a relatively high reversible capacity, as shown by sample A-5 (Table 3). However, the reversible capacity is not as high, as expected from the high first charge capacity for some of the surface modified samples (such as sample

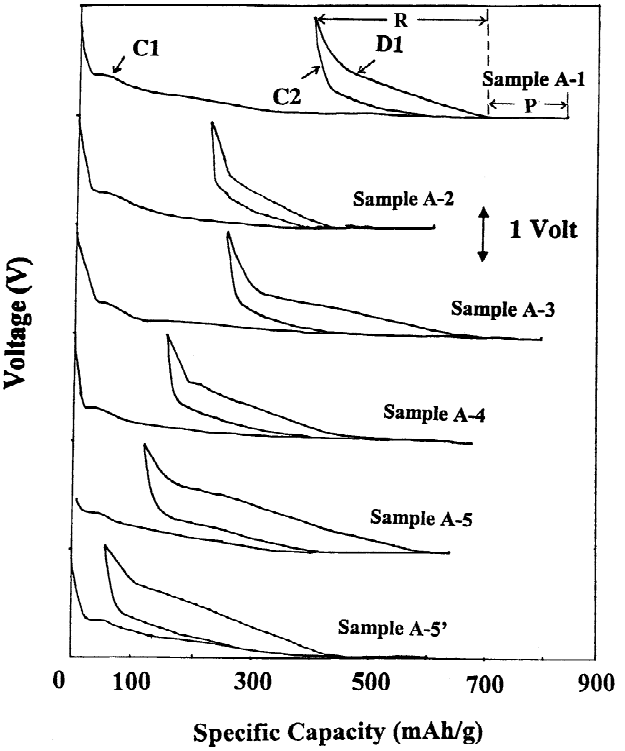

Fig. 3. Characteristics during first charge (C1), first discharge (D1) and second charge (C2) for Samples A-1, A-2, A-3, A-4, A-5 and A-5′. P denotes the Li plating region. R denotes the reversible capacity.

Table 3
First charge/discharge capacities of carbons based on pitch A

Sample no.	Charge/discharge capacity (mAh g^{-1})	Total capacity loss (%)	Reversible capacity (mAh g^{-1})
A-1	832/452	46	320
A-2	594/358	40	220
A-3	789/521	34	440
A-4	674/512	24	360
A-5	643/501	20	480
A-5′	601/514	14	380

A-4), due to the lithium plating. The high reversible capacity obtained for sample A-5 is partly due to the limited lithium plating for this sample.

Table 4 compares the first charge/discharge capacities of carbons based on pitch A and pitch B. As shown in Table 1, these two groups of carbon mainly differ in L_c. Carbons based on pitch A exhibit lower L_c than those based on pitch B. The carbons based on pitch A exhibit higher values of the total capacity loss than those based on pitch B, while the charge capacities are similar. This suggests that a larger L_c may be favorable for reducing the total capacity loss.

Table 5 shows the effect of degassing (step (i) described in Section 2) on the first charge/discharge capacities for carbons based on pitch A. Degassing reduces the total capacity loss; the decrease is particularly large for samples that have been activated (samples A-3, A-4 and A-5).

Table 6 shows the effect of the binder in the carbon anode on the first charge/discharge capacities for carbons based on pitch A. The use of the PVDF binder in place of the teflon binder increases the charge and discharge capacities and decreases the total capacity loss. These effects are quite significant when the carbon has been activated (sample A-3). This is probably because of the

Table 4
Comparison of the first charge/discharge capacities of carbons based on pitch A and pitch B

Sample no.	Charge capacity (mAh g^{-1})	Discharge capacity (mAh g^{-1})	Total capacity loss (%)
A-1	832	452	46
B-1	832	486	42
A-2	594	358	40
B-2	597	389	35
A-3	789	521	34
B-3	794	562	29
A-4	674	512	24
B-4	678	529	22
A-5	643	514	21
B-5	643	539	16

Table 5
Effects of degassing on the first charge/discharge capacities

Sample no.	1st charge capacity (mAh g^{-1})			1st discharge capacity (mAh g^{-1})			Total capacity loss (%)		
	Without degassing	With degassing	Change (%)	Without degassing	With degassing	Change (%)	Without degassing	With degassing	Change (%)
A-1	832	832	0	452	453	0.2	46	46	0
A-2	594	597	0.5	358	362	1	40	40	0
A-3	789	795	0.7	521	572	10	34	28	−18
A-4	674	678	0.5	512	539	5	24	20	−17
A-5	643	645	0.3	501	521	4	21	19	−9

Table 6
Effect of the binder (teflon vs. PVDF) in the carbon anode on the first charge/discharge capacities

Sample no.	1st charge capacity (mAh g^{-1})			1st discharge capacity (mAh g^{-1})			Total capacity loss (%)		
	Teflon	PVDF	Change (%)	Teflon	PVDF	Change (%)	Teflon	PVDF	Change (%)
A-1	832	847	1.8	452	466	3.2	46	45	−2
A-2	594	606	2.1	358	371	3.6	40	38	−5
A-3	789	830	5.2	521	567	8.9	34	32	−6

high surface oxygen concentration after activation (Table 1) affecting the affinity between carbon and binder. That PVDF is superior to teflon as a binder is a finding that is not well understood presently.

4. Conclusion

The charge/discharge performance of Li-ion cells involving a pitch-based carbon anode depends much on the structure and surface composition of the carbon. A high degree of graphitization (as attained by using a high heat-treatment temperature), a decreased concentration of surface oxygen (as attained by reduction in H_2) and a large L_c help to reduce the total capacity loss. Degassing of the carbon and the use of the PVDF binder in place of the teflon binder also help, particularly if the carbon has been activated.

References

[1] Buiel E, George AE, Dahn JR. On the reduction of lithium insertion capacity in hard-carbon anode materials with increasing heat-treatment temperature. J Electrochem Soc 1998;145(7):2252–7.
[2] Buiel E, Dahn JR. Reduction of the irreversible capacity in hard-carbon anode materials prepared from sucrose for Li-ion batteries. J Electrochem Soc 1998;145(6):1977–81.
[3] Arora P, White RE. Capacity fade mechanisms and side reactions in lithium-ion batteries. J Electrochem Soc 1998;145(10):3647–67.
[4] Wu Y, Fang S, Ju W, Jiang Y. Improving the electrochemical properties of carbon anodes in lithium secondary batteries. J Power Sources 1998;70(1):114–7.
[5] Han Y-S, Yu J-S, Park G-S, Lee J-Y. Effects of synthesis temperature on the electrochemical characteristics of pyrolytic carbon for anodes of lithium-ion secondary batteries. J Electrochem Soc 1999;146(11):3999–4004.
[6] Endo M, Kim C, Karaki T, Nishimura Y, Matthews MJ, Brown SDM, Dresselhaus MS. Anode performance of a Li ion battery based on graphitized and B-doped milled mesophase pitch-based carbon fibers. Carbon 1999;37:561–8.
[7] Suzuki K, Iijima T, Wakihara M. Electrode characteristics of pitch-based carbon fiber as an anode in lithium rechargeable battery. Electrochim Acta 1999;4:2185–91.
[8] Nishimura K, Kim YA, Matushita T, Hayashi T, Endo M. Structural characterization of boron-doped submicron vapor-grown carbon fibers and their anode performance. J Mater Res 2000;15(6):1303–13.
[9] Zhou P, Papanek P, Bindra C, Lee R, Fischer JE. High capacity carbon anode materials: structure, hydrogen effect, and stability. J Power Sources 1997;68:296–300.
[10] Yoshio M, Wang H, Fukuda K, Hara Y, Adachi Y. Effect of carbon coating on electrochemical performance of treated natural graphite as lithium-ion battery anode material. J Electrochem Soc 2000;147(4):1245–50.
[11] Zhou P, Lee R, Claye A, Fischer JE. Layer disorder in carbon anodes. Carbon 1998;36(12):1777–81.
[12] Lu W, Chung DDL. Anodic performance of vapor-deprived carbon filaments in lithium-ion secondary battery. Carbon 2001;39(4):493–6.
[13] Zheng T, Liu Y, Fuller EW, Tseng S, von Sacken U, Dahn JR. Lithium insertion in high capacity carbonaceous materials. J Electrochem Soc 1995;142(8):2581–90.